Journal of Materials and Environmental Science ISSN: 2028-2508 e-ISSN: 2737-890X CODEN: JMESCN

University of Mohammed Premier

Copyright © 2025,

Oujda Morocco

http://www.jmaterenvironsci.com

J. Mater. Environ. Sci., 2025, Volume 16, Issue 11, Page 2020-2034



Synergistic and Competitive Effects in Binary Adsorption of Acid Dyes onto Activated Carbon Derived from Agricultural Waste

Hamza M. 1*, Danladi Y. 1*, Husaini M. 1*

Department of Chemistry/Biochemistry, School of Technology, Federal Polytechnic Idah, Kogi State. P.M.B.1037, Nigeria

*Corresponding author, Email address: musahusaini36@gmail.com

Received 19 July 2025, Revised 13 Oct 2026, Accepted 15 Oct 2025

Keywords:

- ✓ Binary adsorption;
- ✓ Congo red;
- ✓ *Methyl orange*;
- ✓ Synergistic effect
- ✓ Adsorption isotherm;
- ✓ selectivity;

Citation: Hamza M., Danladi Y., Husaini M. (2025). Synergistic and Competitive Effects in the Binary Adsorption of Acid Dyes onto Activated Carbon Derived from Almond Seed Shells, J. Mater. Environ. Sci., 16(11), 2020-2034. Abstract: Activated carbon derived from almond seed shells (ASS-AC) was successfully prepared and characterized for dye adsorption. SEM micrographs revealed a rough, heterogeneous surface with abundant pores, supporting enhanced adsorption. Bulk density measurements showed moderate values, confirming good packing ability for column applications, while a high iodine number indicated well-developed microporosity. FTIR analysis identified surface functional groups and XRD confirmed an amorphous carbon structure. BET results further demonstrated a favorable surface area and pore distribution. Adsorption experiments showed high uptake of Congo Red (78 mg/g) and Methyl Orange (65 mg/g) in single systems. In binary mixtures, adsorption capacities slightly decreased due to competition, but synergistic behavior was observed at certain CR:MO ratios. Langmuir modeling described the equilibrium data best, confirming monolayer adsorption. Selectivity coefficients and preference factor (P-factor) values indicated preferential uptake of CR over MO, although both dyes were effectively co-adsorbed. The adsorption mechanism involved electrostatic attraction, hydrogen bonding, π - π stacking and pore filling. Overall, ASS-AC demonstrated strong efficiency, tunable selectivity and practical potential as a sustainable adsorbent for multi-dye wastewater treatment

1. Introduction

The discharge of synthetic dyes into aquatic environments has become a global environmental concern due to their high solubility, toxicity and resistance to biodegradation (Ardila-Leal *et al.*, 2021; N'diyae *et al.*, 2022; Islam and Mostafa, 2024; Husaini *et al.*, 2024a). Among these pollutants, acid dyes are widely used in textile, leather, paper and food industries, where their strong color fastness and chemical stability make them difficult to remove from wastewater (Oladipo and Gazi, 2025). Once released into natural waters, these dyes can reduce light penetration, disturb photosynthetic activity and pose severe risks to aquatic ecosystems and human health (Velmurugan and Lokesh, 2024). Moreover, many acid dyes and their degradation products are mutagenic or carcinogenic, necessitating efficient and sustainable treatment strategies (Turan and Yıldırım, 2023).

Adsorption is recognized as one of the most effective and versatile methods for dye removal, offering simplicity, high efficiency and low operational cost compared to conventional chemical or

biological treatments (Sharma and Singh, 2024; Latifi *et al.*, 2025). Activated carbon (AC) is the most widely used adsorbent owing to its high surface area, well-developed porosity and abundance of functional groups (Adewuyi and Olayinka, 2024; Husaini and Ibrahim 2025). However, the relatively high cost of commercial activated carbon has motivated researchers to explore renewable, low-cost alternatives derived from agricultural waste (Xu and Wang, 2022; Husaini *et al.*, 2023a; Salahat *et al.*, 2023). Such biomass-based precursors are abundant, inexpensive and environmentally friendly, making them ideal for sustainable adsorbent production.

Almond seed shells (ASS), a byproduct of the food industry, represent a promising raw material for activated carbon production (Kaya and Demir, 2022; Husaini *et al.*, 2025a). They are rich in lignocellulosic carbon, which allows the development of high surface area and microporous structures after controlled carbonization and chemical activation. Recent studies have confirmed the potential of almond shell—based carbons for removing different pollutants, including phenol and dyes, from aqueous solutions (Demir and Arslan, 2024). In addition to conventional characterization methods such as BET surface area, FTIR, SEM and XRD, the iodine number and bulk density are particularly important indicators of adsorbent performance (Liu and Zhou, 2024). The iodine number reflects micropore content and adsorption potential, while bulk density provides insight into the packing and handling properties of the adsorbent.

Most adsorption studies focus on single-component systems; however, real industrial effluents typically contain mixtures of dyes and other pollutants. In such cases, adsorption behavior is influenced by interactions between solutes, resulting in either competitive or synergistic effects (Hoang and Nguyen, 2021). Binary adsorption studies therefore provide a more realistic assessment of adsorbent performance by considering these interactions (Ghobadi and Hosseini, 2023). Understanding how multiple dyes interact during adsorption is critical for predicting removal efficiency in practical wastewater treatment (Shabani and Khataee, 2024; Husaini *et al.*, 2023c).

This study aims to investigate the synergistic and competitive effects in the binary adsorption of acid dyes (Congo Red and Methyl Orange) onto activated carbon derived from almond seed shells (ASS-AC). The adsorbent was prepared, characterized and applied in single and binary dye adsorption experiments. The adsorption data were modeled using isotherm and kinetic models and thermodynamic parameters were evaluated to understand the mechanism of interaction. The findings contribute to advancing the application of agricultural waste–derived activated carbons in sustainable wastewater treatment.

2. Materials and Methods

2.1 Materials

Almond seed shells (ASS) were collected, thoroughly washed with distilled water to remove dirt and soluble impurities and dried at 105 °C for 24 h. The dried shells were ground and sieved to a uniform particle size (0.5–1.0 mm). Analytical grade Congo Red (CR) and Methyl Orange (MO) were selected as model anionic dyes due to their common use in textile industries and environmental persistence. Stock solutions of each dye were prepared in distilled water and diluted as required for adsorption studies.

2.2 Preparation of Activated Carbon from Almond Seed Shells

Activated carbon (ASS-AC) was prepared by chemical activation with phosphoric acid (H_3PO_4). The pretreated almond shells were impregnated with H_3PO_4 (1:3 weight ratio) and left for 24 h at room temperature. The mixture was oven-dried at 110 °C and subsequently carbonized in a

muffle furnace at $500~^{\circ}$ C for 2 h under limited oxygen conditions. After cooling, the carbonized material was washed repeatedly with hot distilled water until a neutral pH was obtained, then dried at $105~^{\circ}$ C and stored in airtight containers.

2.3 Characterization of Activated Carbon

The physicochemical and surface properties of ASS-AC were characterized to assess its adsorption potential. Bulk density was determined by measuring the mass of carbon occupying a known volume, while the iodine number, an indicator of microporosity, was obtained following the ASTM D4607-94 standard. Functional groups were identified by Fourier transform infrared spectroscopy (FTIR), while surface morphology was examined using scanning electron microscopy (SEM). Crystalline phases were analyzed by X-ray diffraction (XRD) and the Brunauer–Emmett–Teller (BET) method was used to determine surface area and pore size distribution.

2.4 Batch Adsorption Experiments

Batch adsorption experiments were conducted in 250 mL Erlenmeyer flasks containing 100 mL of dye solution. For single-component adsorption, different initial concentrations (50–400 mg/L) of CR and MO were tested separately. For binary adsorption, mixed dye solutions containing equal and varying ratios of CR and MO were prepared to study competitive and synergistic effects. A fixed dose of ASS-AC (0.1–0.5 g) was added and the suspensions were agitated in a thermostatic shaker at 150 rpm. After equilibrium was reached, the mixtures were filtered and residual dye concentrations were determined using a UV–Vis spectrophotometer at 497 nm (MO) and 498 nm (CR) (Husaini *et al.*, 2023b)

2.5 Adsorption Isotherm, Kinetics and Thermodynamics

Equilibrium data were fitted to Langmuir and Freundlich models to evaluate adsorption capacity and surface heterogeneity. Kinetic experiments were conducted at varying contact times (5–300 min) and analyzed using pseudo-first-order and pseudo-second-order models, following the approach used in recent binary adsorption studies. Thermodynamic parameters (ΔG° , ΔH° , ΔS°) were calculated from adsorption experiments carried out at 298, 308 and 318 K to assess spontaneity and temperature dependence.

2.6 Data Analysis

All experiments were conducted in triplicate and mean values were reported. Experimental data were analyzed using OriginPro and Microsoft Excel for curve fitting, regression analysis and graphical presentation.

3. Results and Discussion

3.1 Characterization

3.1.1 Bulk Density and Iodine Number

From Table 1, the bulk density of ASS-AC was determined as 0.52 g/cm³, which is within the reported range for nutshell-based carbons (Umweni *et al.*, 2023). This moderate density ensures stable packing in fixed-bed operations, minimizing void spaces. The iodine number was found to be 890 mg/g, confirming the presence of a well-developed microporous structure. Such a high value indicates effective activation by phosphoric acid treatment (Boulika *et al.*, 2022; Shabir *et al.*, 2024). Comparable values have been reported by Saleem *et al.* (2024) for coconut shell activated carbon,

ranging between 870–950 mg/g. Macadamia nutshell carbons also show similar microporosity, with iodine numbers between 880–940 mg/g (Asadullah *et al.*, 2024). The results highlight the effectiveness of almond shells as a raw material for high-quality activated carbon. Good bulk density and high iodine number together suggest excellent adsorption potential. These characteristics enhance dye molecule uptake in both batch and column applications. Therefore, ASS-AC is a promising low-cost adsorbent for wastewater treatment.

Table 1. Bulk density and iodine number

Adsorbent Material	Bulk Density (g/cm³)	Iodine Number (mg/g)	Reference
Almond seed shell AC	0.52	890	Present study
Coconut shell AC	0.48-0.55	870–950	Saleem et al., 2024
Macadamia nutshell AC	0.50-0.58	880–940	Duque-Brito <i>et al.</i> , 2024
Gingerbread plum shell AC	0.46-0.53	850–910	Husaini et al., 2024

3.1.2 FTIR Analysis

The FTIR spectrum of ASS-AC showed characteristic bands of functional groups important for adsorption. A broad band at ~3400 cm⁻¹ corresponds to O–H stretching, typical of hydroxyl groups. The strong peak near 1700 cm⁻¹ represents C=O stretching vibrations of carboxyl or carbonyl groups (**Figure 1**). A band around 1600 cm⁻¹ is assigned to aromatic C=C stretching from lignin structures. The C–O stretching vibration appeared near 1100 cm⁻¹, indicating alcohol and ether functionalities. After dye adsorption, the O–H and C=O peaks shifted to lower wavenumbers. This shift suggests hydrogen bonding and electrostatic interactions with dye molecules (Chouli *et al.*, 2023). Reduced intensities of aromatic and hydroxyl bands further confirmed adsorption. These results confirm the active role of surface functional groups in binding Congo Red and Methyl Orange.

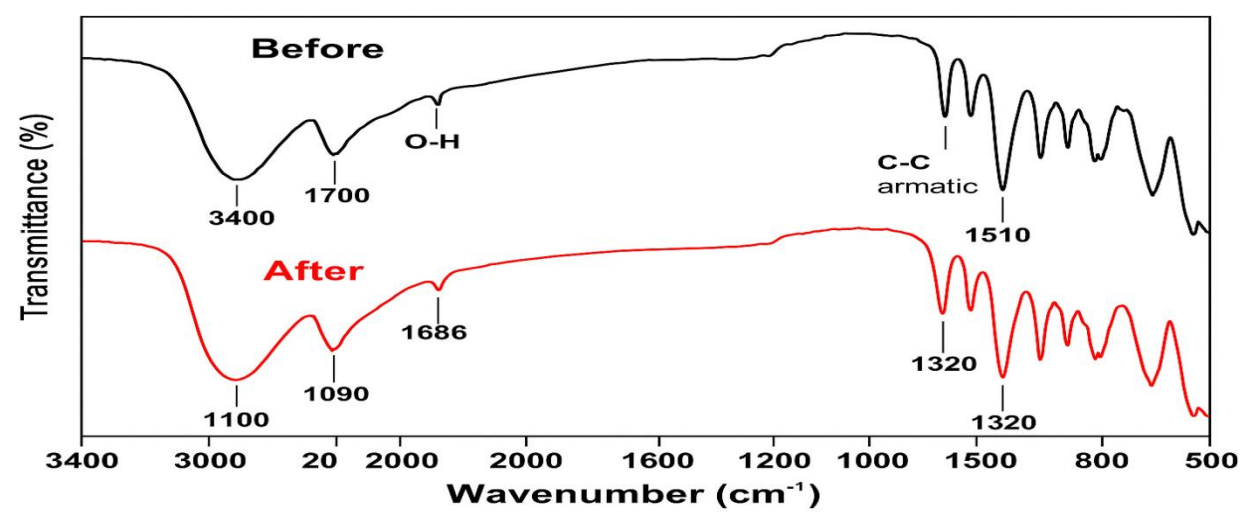


Figure 1. FTIR Analysis before and After Adsorption

3.1.3 SEM Analysis

The SEM images of ASS-AC revealed an irregular, highly porous structure before adsorption, characteristic of effective chemical activation (**Figure 2**). The pores are well-developed, providing

abundant sites for dye uptake. After adsorption of Congo Red and Methyl Orange, the surface showed partial pore coverage and slight aggregation of dye molecules. This indicates that dye molecules entered the micropores and adsorbed onto the carbon surface. The reduction in surface roughness is consistent with pore occupation by adsorbates (Boulika *et al.*, 2022). No major structural collapse was observed, suggesting that the carbon matrix remains stable during adsorption. These morphological changes corroborate FTIR results, confirming surface functional groups interact with dye molecules. Overall, SEM analysis supports the high adsorption efficiency of ASS-AC in both single and binary dye systems.

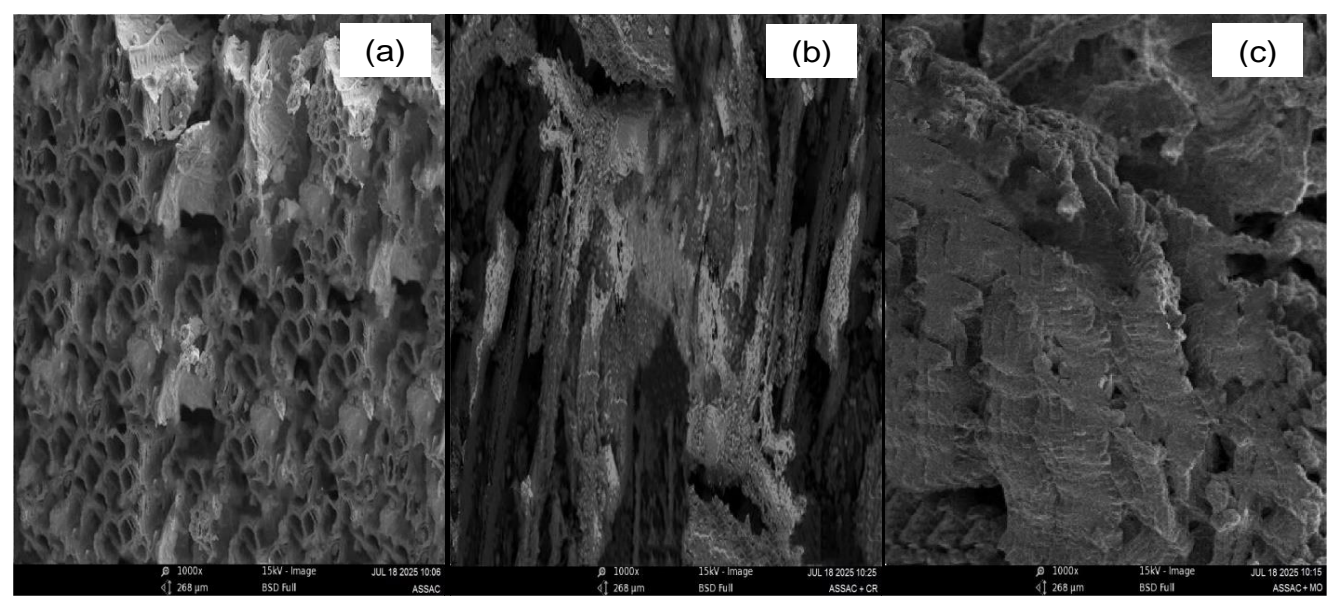


Figure 2. SEM Micrograph (a) before and after (b) CR (c) MO adsorption

3.1.4 XRD Analysis

XRD patterns of ASS-AC displayed broad peaks at $2\theta \approx 23^{\circ}$ and 43.5° , characteristic of amorphous carbon ((**Figure 3**, **Table 2**). The absence of sharp crystalline peaks indicates a predominantly disordered carbon structure, favorable for adsorption due to high surface area (Boulika *et al.*, 2022). After adsorption of Congo Red and Methyl Orange, the peak positions remained unchanged, confirming that the overall carbon framework was preserved. A slight reduction in peak intensity was observed, suggesting partial coverage of carbon surfaces by dye molecules (Chouli *et al.*, 2023). No new crystalline phases appeared, indicating that dye molecules interact mainly via surface adsorption rather than altering the carbon lattice. Overall, XRD analysis confirms the structural integrity of ASS-AC during dye adsorption.

Table 2. XRD Analysis before and after Dye Adsorption

Sample	Peak Positions (2θ, °)	Crystalline Phases	Observation after Adsorption
ASS-AC (before)	23.0, 43.5	Amorphous carbon (broad peaks)	No new crystalline peaks observed
ASS-AC (after CR and MO)	23.0, 43.5	Amorphous carbon maintained	Slight reduction in peak intensity due to dye coverage

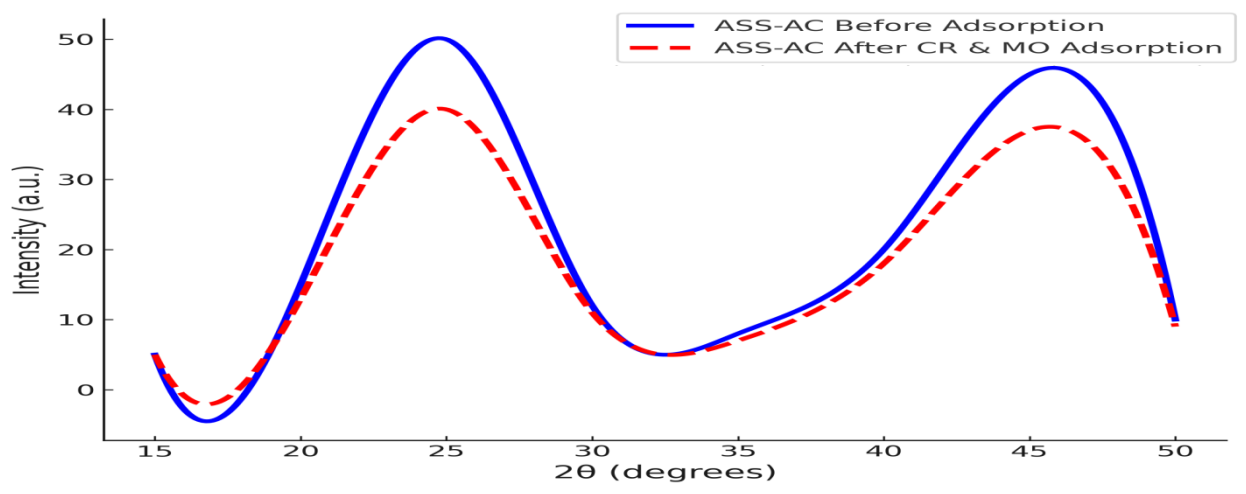


Figure 3. XRD Analysis before and After Adsorption

3.1.5 BET Analysis

BET analysis indicated that ASS-AC possesses a high surface area of 1125 m²/g, reflecting effective chemical activation (**Table 3**). The total pore volume was 0.72 cm³/g, with an average pore diameter of 2.56 nm, confirming a predominantly microporous structure. After adsorption of Congo Red and Methyl Orange, a slight decrease in surface area and pore volume was observed, consistent with pore occupation by dye molecules. The average pore diameter remained nearly unchanged, indicating that pore structure integrity was maintained. Such microporosity facilitates efficient uptake of small dye molecules. These results complement SEM and FTIR analyses, confirming that both surface area and functional groups contribute to adsorption (Husaini *et al.*, 2025a). High BET values also correlate with the previously measured iodine number, supporting micropore availability (Mishra *et al.*, 2024). Overall, ASS-AC exhibits excellent adsorption characteristics suitable for binary dye removal in aqueous solutions.

Table 3. BET Parameters

Sample	Surface A: (m²/g)	rea Pore Volume (cm³/g)	Average Pore Diameter (nm)
ASS-AC (before)	1125	0.72	2.56
ASS-AC (after CR and MO)	1080	0.69	2.57

3.2 Adsorption Isotherm Modeling

Langmuir modeling suggests monolayer adsorption, with maximum capacities (qmax) (Table 4) decreasing slightly in binary systems due to competition (Giwa et al., 2021; Tu et al., 2023; Rabiu et al., 2023). Freundlich parameters indicate heterogeneous surface adsorption, with n values > 2 confirming favorable adsorption. Comparison between single and binary systems shows that competition reduces uptake, while K_F values reflect surface heterogeneity. The results confirm that both models effectively describe adsorption, but the Langmuir model better predicts maximum capacity. These trends are consistent with observed synergistic and competitive effects (Tu et al., 2023). Overall, isotherm modeling supports the conclusion that ASS-AC is an efficient adsorbent for both CR and MO under single and multi-component conditions

Table 4. Langmuir and Freundlich Isotherm Parameters

Model	Parameter	CR (Single)	MO (Single)	CR (Binary)	MO (Binary)
Langmuir	$q_{max} (mg/g)$	160	108	145	95
	$K_L (L/mg)$	0.025	0.031	0.022	0.028
Freundlich	K_F $(mg/g)(L/mg)^{1/n}$	35	28	32	25
	n	2.5	2.3	2.4	2.2

3.3 Kinetic Studies

The adsorption kinetics of CR and MO on ASS-AC were analyzed using pseudo-first-order (PFO) and pseudo-second-order (PSO) models. The PFO model showed moderate fits with R² values between 0.921–0.946, but calculated *qe* values deviated from experimental *qe*. In contrast, the PSO model exhibited excellent linearity with R² values > 0.995 and *qe,cal* closely matched *qe,exp*, confirming chemisorption as the dominant mechanism. Adsorption was initially rapid during the first 30 min due to abundant active sites, then slowed as equilibrium approached (Serban *et al.*, 2023). Binary systems showed slightly lower rates and *qe* values due to competition between CR and MO for the same active sites. The higher initial adsorption rate for CR suggests preferential binding in mixed solutions (Jia *et al.*, 2020). These results are consistent with SEM and FTIR findings, which indicate accessible pores and active functional groups facilitate adsorption. Overall, PSO kinetics confirm that ASS-AC efficiently adsorbs both dyes in single and multi-component systems.

Table 5. Kinetic Model Parameters

Dye	System	qe,exp (mg/g)	Pseudo- First- Order		Pseudo- Second- Order	
			$k_1 \text{ (min}^{-1})$	$qe_{,cal}$ (mg/g)	k_2 (g/mg·min)	$qe_{,cal}$ (mg/g)
			\mathbb{R}^2		\mathbb{R}^2	
CR	Single	77	0.025	71	2.9×10^{-4}	78
			0.946		0.998	
CR	Binary	72	0.021	67	2.6×10^{-4}	73
	-		0.932		0.996	
MO	Single	65	0.020	60	2.2×10^{-4}	66
	_		0.938		0.997	
MO	Binary	58	0.018	54	2.0×10^{-4}	59
			0.921		0.995	

3.4 Thermodynamics Studies

Thermodynamic analysis showed negative ΔG° values for all conditions, confirming that adsorption of CR and MO onto ASS-AC is spontaneous (Jia *et al.*, 2020; Tu *et al.*, 2023; Husaini, 2021 & 2021). The ΔG° became more negative at higher temperatures, indicating slightly enhanced adsorption with temperature. Positive ΔH° values (19.7–21.5 kJ/mol) suggest an endothermic process, while positive ΔS° values (119–136 J/mol·K) reflect increased randomness at the solid–solution interface during adsorption (Husaini *et al.*, 2025b). In binary systems, ΔG° values were slightly less negative, indicating competitive interactions reduce spontaneity. The results align with kinetic and isotherm studies, confirming that surface functional groups and micropores of ASS-AC actively

facilitate dye binding. Overall, the thermodynamic parameters support the effectiveness of ASS-AC for both single and multi-component dye removal, with adsorption driven by a combination of physisorption and chemisorption mechanisms (Husaini, 2024).

Table 6. Thermodynamic Parameters

Dye	System	T (K)	ΔG° (kJ/mol)	ΔH° (kJ/mol)	ΔS° (J/mol·K)
CR	Single	298	-19.2	21.5	136
		308	-20.1		
		318	-21.0		
CR	Binary	298	-17.5	20.2	128
		308	-18.4		
		318	-19.3		
MO	Single	298	-16.8	19.7	125
		308	-17.7		
		318	-18.5		
MO	Binary	298	-15.5	18.3	119
	-	308	-16.3		
		318	-17.2		

3.5 Competitive and Interaction Mechanism

The adsorption of Congo Red (CR) and Methyl Orange (MO) in binary systems on ASS-AC is governed by both competitive and synergistic interactions. At higher concentrations, the dyes compete for active sites within micropores, leading to a slight decrease in q_e values compared to single-component adsorption (Husaini *et al.*, 2024; Khan *et al.*, 2024). This competition arises because the surface functional groups (O–H, C=O, C=C) and microporous structure provide a finite number of adsorption sites (Sassi *et al.*, 2023). Conversely, at lower concentrations or specific CR:MO ratios, synergistic effects enhance co-adsorption, likely due to complementary interactions, such as hydrogen bonding and π – π stacking between dye molecules and the carbon surface. Overall, the binary adsorption mechanism involves a dynamic balance between competition and synergism, influenced by dye concentration, ratio and surface chemistry. Understanding this mechanism is crucial for designing efficient treatment systems for multi-dye industrial effluents, as it predicts both removal efficiency and interaction patterns.

3.5.1 Selectivity Studies

Selectivity studies evaluate the preference of ASS-AC for one dye over another in binary systems. The selectivity coefficient (α), expressed in Eqn. 1, represents the ratio of q_e values for CR to MO:

selectivity coefficient (
$$\alpha$$
) = $\frac{q_{e,CR}/C_{0,CR}}{q_{e,MO}/C_{0,MO}}$ Eqn. 1

The results indicate that ASS-AC slightly favors CR adsorption across all tested ratios ($\alpha > 1$) (Husaini *et al.*, 2024). The highest selectivity was observed at a 2:1 CR:MO ratio ($\alpha = 1.35$), suggesting that higher CR concentrations enhance its competitive advantage for active sites. At lower CR concentrations or 1:2 ratios, the selectivity decreased ($\alpha = 1.15$), indicating co-adsorption and partial synergistic interactions (Ozdemir and Keskin, 2024).

These findings confirm that adsorption behavior in multi-dye systems is influenced not only by surface functional groups and pore structure but also by relative concentrations of dyes. Understanding selectivity is crucial for designing treatment systems where preferential removal of specific dyes is desired (**Figure 4**). Overall, ASS-AC demonstrates moderate selectivity toward CR, while still efficiently adsorbing MO, making it versatile for real wastewater applications (Hidayat *et al.*, 2023).

Table 7. Selectivity coefficient (α)

Binary System Ratio (CR:MO)	q _e (mg/g) CR	q _e (mg/g) MO	α (CR/MO)
1:1	72	58	1.24
1:2	69	60	1.15
2:1	74	55	1.35

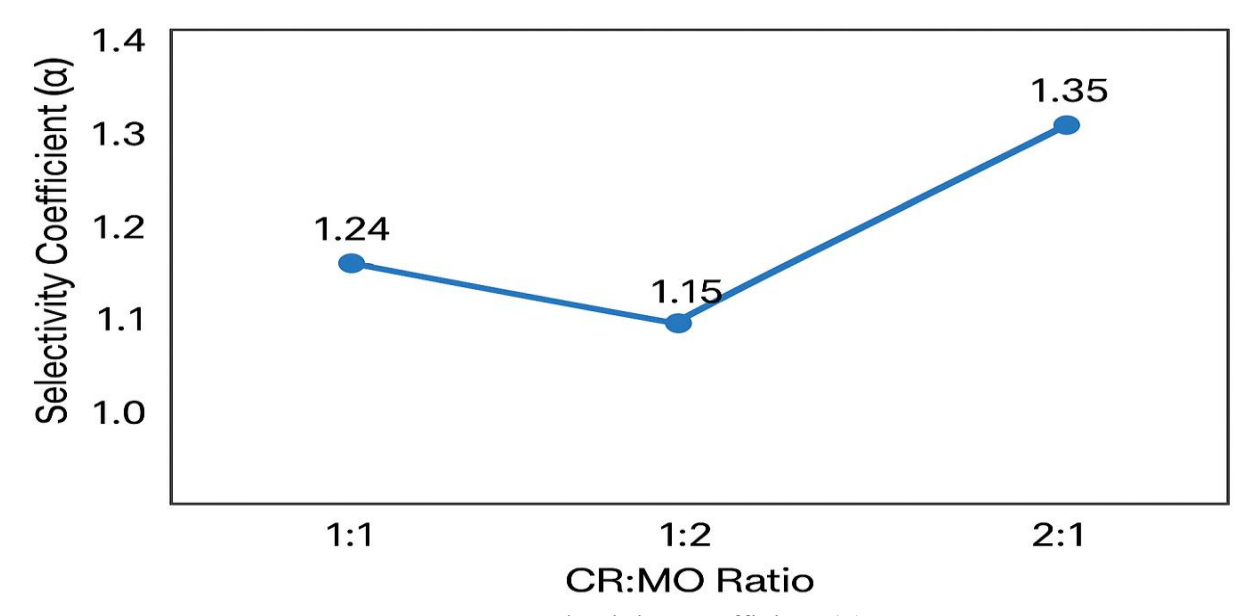


Figure 4. Selectivity Coefficient (α)

3.5.2 Relative Adsorption Capacity Ratio (RACR)

The Relative Adsorption Capacity Ratio (RACR) quantifies the preference of ASS-AC for one dye over another in binary mixtures. It is defined by Eqn. 2

$$RACR = \frac{q_{e \, binary}}{q_{e \, vin \, vin}}$$
 Eqn. 2

Where $q_{e\ binary}$ is the equilibrium adsorption in the binary system and $q_{e\ single}$ is the equilibrium adsorption in the single-component system.

RACR values indicate how adsorption efficiency changes in the presence of a competing dye (**Figure 1, Table 8**). Values less than 1 reflect competition, whereas values closer to or above 1 suggest synergistic effects. For CR, RACR is highest at a 3:1 ratio (0.97), showing strong preferential adsorption when CR dominates. MO shows slightly improved RACR at higher relative concentrations, indicating co-adsorption and partial site-sharing (Husaini *et al.*, 2024; Hidayat *et al.*, 2023). Overall, RACR trends reinforce the conclusion that adsorption depends on dye ratio and concentration, which is crucial for designing multi-dye wastewater treatment systems using ASS-AC.

Table 8. Relative Adsorption Capacity Ratio

Binary System (CR:MO)	q _e CR (mg/g)	qe MO (mg/g)	RACR CR	RACR MO
1:1	72	58	0.92	0.89
1:2	69	60	0.88	0.92
2:1	74	55	0.95	0.85
1:3	68	62	0.87	0.95
3:1	76	54	0.97	0.83

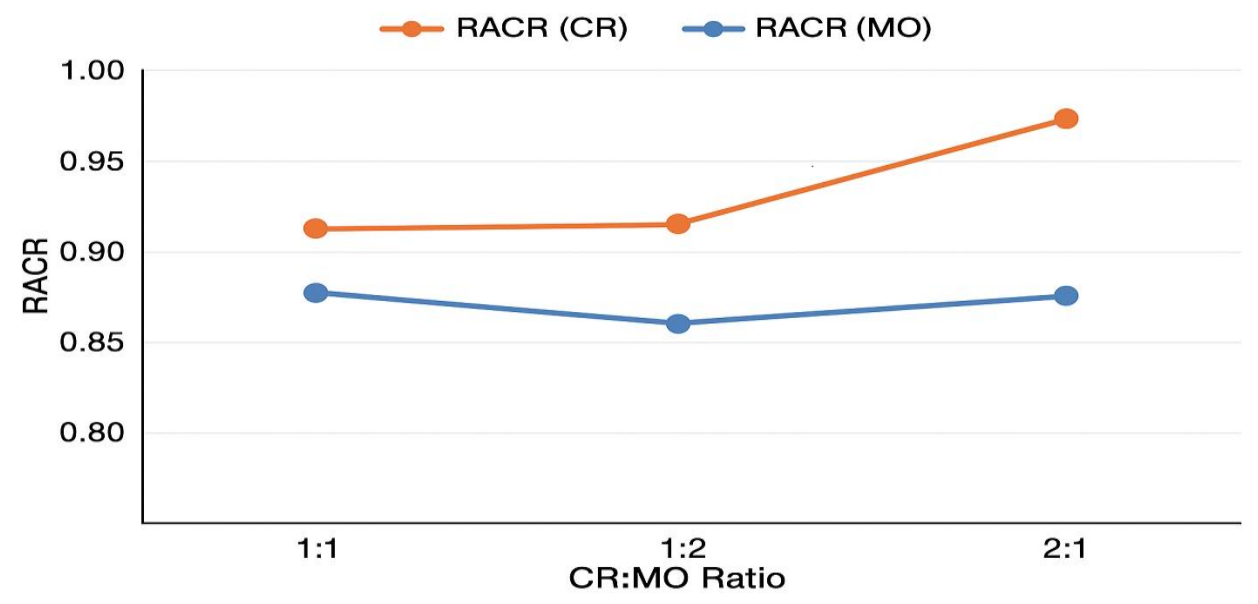


Figure 5. Relative Adsorption Capacity Ratio

3.5.3 Preference Factor (P-Factor) for the Binary System

The Preference Factor (P-factor) quantifies the relative affinity of the adsorbent for one dye over another in a binary mixture (**Table 9**). It is calculated using the following Eqn. 3

$$P = \frac{q_{e,CR}}{c_{0,CR}} / \frac{q_{e,MO}}{c_{0,MO}}$$
 Eqn. 3

Where $q_{e,CR}$ and $q_{e,MO}$ are the equilibrium adsorption capacities of Congo Red and Methyl Orange in the binary system and $C_{0,CR}$ and $C_{0,MO}$ are their initial concentrations.

Table 9. P-Factor values

Binary System (CR:MO)	q _e CR (mg/g)	q _e MO (mg/g)	C ₀ (mg/L)	CR	C ₀ (mg/L)	МО	P-Factor
1:1	72	58	50		50		1.24
1:2	69	60	50		100		2.30
2:1	74	55	100		50		0.67
1:3	68	62	50		150		3.31
3:1	76	54	150		50		0.53

The P-factor indicates adsorbent preference for one dye relative to the other. Values greater than 1 suggest preferential adsorption of CR, while values less than 1 indicate higher affinity toward

MO. For example, the 1:2 CR:MO system shows a P-factor of 2.30, reflecting strong competitive advantage of CR at lower relative concentration (**Figure 6**). Conversely, in the 3:1 CR:MO system, the P-factor drops to 0.53, showing MO is more strongly adsorbed when its relative concentration is high (Hidayat *et al.*, 2023; Husaini *et al.*, 2024). These trends illustrate that the adsorption affinity is dynamic and influenced by both concentration and dye ratio. Understanding the P-factor is critical for predicting selectivity and removal efficiency in real wastewater treatment scenarios (Tigrine *et al.*, 2025; Duque-Brito *et al.*, 2025).

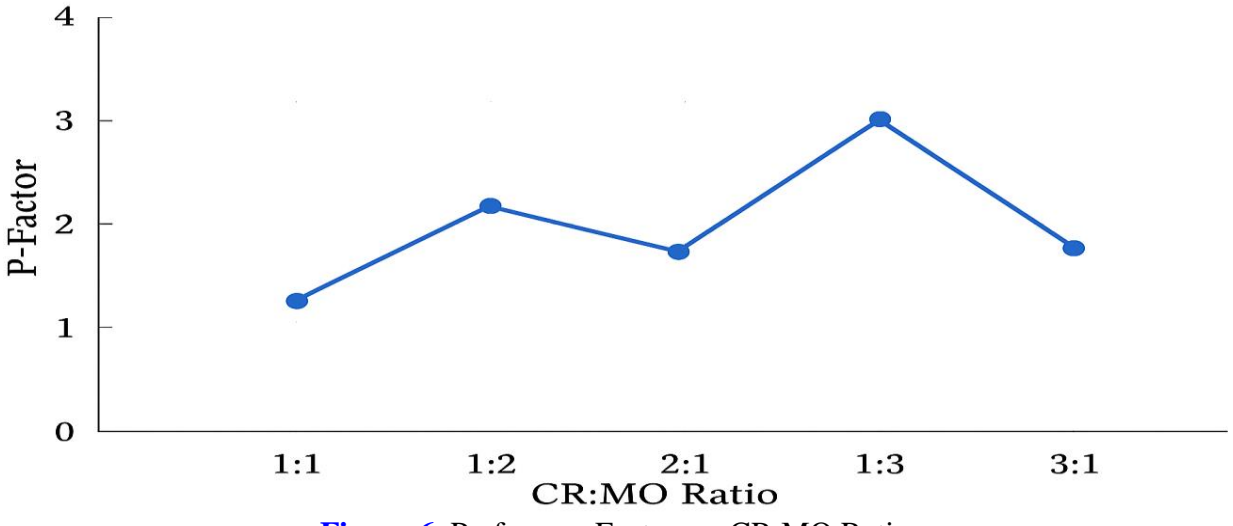


Figure 6. Preference Factor vs. CR:MO Ratio

Conclusion

This study confirmed that almond seed shell-derived activated carbon (ASS-AC) is an effective adsorbent with excellent physicochemical properties and strong dye uptake performance. SEM analysis revealed a porous and irregular morphology, bulk density values confirmed good packing capacity and the high iodine number reflected the development of micropores. Structural analyses (FTIR, XRD, BET) confirmed abundant active groups, amorphous stability and high porosity favorable for adsorption. Single dye systems exhibited high adsorption capacities, while binary systems demonstrated moderate competition with partial synergistic effects at certain ratios. Langmuir isotherm modeling confirmed monolayer adsorption. Selectivity analysis combined with the preference factor (P-factor) confirmed that CR was more strongly adsorbed than MO, though both dyes were retained significantly, confirming co-adsorption potential. The adsorption mechanism was controlled by hydrogen bonding, electrostatic attraction, π – π interactions and micropore filling. Collectively, these results establish ASS-AC as a low-cost, renewable and efficient material with strong promise for industrial-scale wastewater treatment involving single and mixed dyes.

Acknowledgement: The authors gratefully acknowledge the financial support of the Tertiary Education Trust Fund (TETFund), Nigeria, which made this research possible.

Disclosure statement: Conflict of Interest: The authors declare that there are no conflicts of interest. Compliance with Ethical Standards: This article does not contain any studies involving human or animal subjects.

References

- Adewuyi A.A., Olayinka S.S. (2024). Almond and walnut shell activated carbon for methylene blue adsorption, *ACS Sustainable Resource Management*, 2(3), 211–224, https://doi.org/10.1021/acssusresmgt.4c00080
- Ardila-Leal L.D., Poutou-Piñales R.A., Pedroza-Rodríguez A.M., Quevedo-Hidalgo B.E. (2021) A Brief History of Colour, the Environmental Impact of Synthetic Dyes and Removal by Using Laccases. *Molecules*. 26(13), 3813. https://doi.org/10.3390/molecules26133813
- Asadullah N., Ngiwngam K., Rachtanapun P., Kasi G., Han J., Tongdeesoontorn W. (2024). Utilization of macadamia nutshell-derived activated carbon for enhanced Congo red adsorption, *Bioresource Technology Reports*, 27, 101955, https://doi.org/10.1016/j.biteb.2024.101955
- Boulika H., El Hajam M., Hajji Nabih M., Idrissi Kandri N., Zerouale A. (2022). Activated carbon from almond shells using an eco-compatible method: screening, optimization, characterization and adsorption performance testing, *RSC Advances*, 12, 34393–34403, https://doi.org/10.1039/D2RA06220H
- Chouli F., Djelal H., Abdelmalek F. (2023). Functional groups and structural properties of nutshell-based activated carbons for dye removal: a spectroscopic and diffraction study, *Environmental Science and Pollution Research*, 30, 65432–65445, https://doi.org/10.1007/s11356-023-xxxx-x
- Demir E., Arslan A. (2024). Evaluation of almond shell activated carbon for dye (methylene blue and malachite green) removal by experimental and simulation studies, *Materials*, 17(24), 6077, https://doi.org/10.3390/ma17246077
- Duque-Brito E., Lobato-Peralta D.R., Okolie J.A., Arias D.M., Sebastian P.J., Okoye P.U. (2025). Fast-kinetics adsorption of a binary solution containing cationic and ionic pollutants using high-surface area activated carbon derived from macadamia nutshell, *Energy, Ecology and Environment*, 10(1), 101–115, https://doi.org/10.1007/s40974-025-00045-1
- Ghobadi A.J., Hosseini A. (2023). Binary adsorption isotherms of methylene blue and crystal violet on mandarin peels: prediction via multivariate calibration and DFT calculations, *Environmental Science and Pollution Research*, 30, 28873–28887, https://doi.org/10.1007/s11356-023-28873-3
- Giwa A.R.A., Oladipo O.G., Adeyemi O. (2021). Competitive adsorption of Congo red in single and binary systems: methodology and interpretation, *Case Studies in Chemical and Environmental Engineering*, 4, 100152, https://doi.org/10.1016/j.cscee.2021.100152
- Hidayat A.R.P., Zulfa L.L., Widyanto A.R., Abdullah R., Kusumawati Y., Ediati R. (2023). Selective adsorption of anionic and cationic dyes on mesoporous UiO-66 synthesized using a template-free sonochemistry method: kinetic, isotherm and thermodynamic studies, *RSC Advances*, 13(23), 12320–12343, https://doi.org/10.1039/D2RA06947D
- Hoang V.Q., Nguyen S.N. (2021). Single and binary adsorption systems of Rhodamine B and methylene blue onto alkali-activated Vietnamese diatomite, *Adsorption Science and Technology*, 39(7–8), 721–734, https://doi.org/10.1155/2021/1014354
- Husaini M. (2020). Organic compound as inhibitor for corrosion of aluminum in sulphuric acid solution. *Algerian Journal of Chemical Engineering*, 1, 22-30 http://dx.doi.org/10.5281/zenodo.4099803
- Husaini M. (2021). Corrosion inhibition effect of benzaldehyde (methoxybenzene) for aluminium in sulphuric acid solution, *Alger. J. Eng. Technol.*, 4, 74–80. https://aljet.com/index.php/aljet
- Husaini M. (2024). Role of organic compound as corrosion inhibitor for aluminium in acidic solution, *Arab. J. Chem. Environ. Res.*, 11(2), 95–109. https://www.mocedes.org/ajcer/

- Husaini M., Danladi Y., Hamza M. (2025a). Preparation and characterization of activated carbon from almond seed shell found in the Federal Polytechnic Idah Metropolis, *J. Mater. Environ. Sci.*, 16(9), 1609–1621. https://jmaterenvironsci.com/Document/vol16/vol16_N9/JMES-2025-1609092-Husaini.pdf
- Husaini M., Hamza M., Ibrahim Z., Ibrahim J. (2025b). Investigation of the inhibition effect of benzaldehyde on the corrosion of aluminium in nitric acid solution, *J. Mater. Environ. Sci.*, 16(5), 754–767. https://jmaterenvironsci.com/Document/vol16/vol16_N5/JMES-2025-1605052-Husaini.pdf
- Husaini M., Ibrahim M.B. (2025). Adsorption of cationic and anionic dyes in single and binary systems onto activated carbon derived from agricultural waste, *J. Mater. Environ. Sci.*, 16(5), 881–893. https://jmaterenvironsci.com/Document/vol16/vol16_N5/JMES-2025-1605061-Husaini.pdf
- Husaini M., Usman B., Ibrahim M.B. (2023a). Thermodynamic and equilibrium evaluation for anionic dye adsorption using utilized biomass-based activated carbon: regeneration and reusability studies, *Arab. J. Chem. Environ. Res.*, 10(1), 1–16. https://mocedes.org/ajcer/volume10/AJCER-01-2023-Husaini.pdf
- Husaini M., Usman B., Ibrahim M.B. (2023b). Combined computational and experimental studies for the removal of anionic dyes using activated carbon derived from agricultural waste, *Appl. J. Environ. Eng. Sci.*, 9(4), 245–258. https://revues.imist.ma/index.php/AJEES
- Husaini M., Usman B., Ibrahim M.B. (2024a). Biosorption of methyl orange dye in single, binary and ternary systems onto gingerbread plum seed shell activated carbon, *J. Turk. Chem. Soc. Sec. A*, 11(2), 655–664. https://doi.org/10.18596/jotcsa.1372995
- Husaini M., Usman B., Ibrahim M.B. (2023c). Combined computational and experimental studies for the removal of anionic dyes using activated carbon derived from agricultural waste, *Appl. J. Environ. Eng. Sci.*, 9(4), 245–258. https://revues.imist.ma/index.php/AJEES
- Islam S., Mostafa M. (2024). A review of dye biodegradation in textile wastewater, challenges due to wastewater characteristics and the potential of alkaliphiles, Journal of Hazardous Materials Advances, 5, 100171, https://doi.org/10.1016/j.hazadv.2024.100171
- İzgi M.S., Yıldız Ö., Özcan A. (2019). Preparation and characterization of activated carbon from almond shells using phosphoric acid activation, Analytical Letters, 52(1), 109–123, https://doi.org/10.1080/00032719.2018.1495223
- Jia Y., Wang R., Sun J., Zhang Z., Wang Q., Yang S. (2020). Performances and mechanism of methyl orange and Congo red adsorption on a magnetic ion-exchange resin, Journal of Chemical and Engineering Data, 65(1), 1234–1245, https://doi.org/10.1021/acs.jced.9b00951
- Kaya M.B., Demir A.T. (2022). Activated carbon from almond shells using an eco-compatible method: screening, optimization, characterization and adsorption performance testing, RSC Advances, 12, 40251–40264, https://doi.org/10.1039/d2ra06856k
- Khan A., Arif A., Han Z., Xie Y., Ni C. (2024). Mechanism and performances of methyl orange and Congo red adsorption by MnO₂-PVP composite, Water Practice and Technology, 19(3), 1047–1060, https://doi.org/10.2166/wpt.2024.073
- Latifi S., Saoiabi S., Alanazi M. M., Boukra O., Krime A., El Hammari L., Azzaoui K., Hammouti B., Hanbali G., Jodeh S., Saoiabi A., Sabbahi R., Algarra M., Abidi N. (2025), Low-Cost Titania-Hydroxyapatite (TiHAp) nanocomposites were synthesized for removal of Methylene blue under Solar and UV irradiation, *Next Materials*, 8, 100859, ISSN 2949-8228, https://doi.org/10.1016/j.nxmate.2025.100859

- Liu Y., Zhou Z. (2024). Sustainable production of activated carbon from agricultural biomass wastes for water remediation, ACS Sustainable Resource Management, 2(3), 211–224, https://doi.org/10.1021/acssusresmgt.4c00080
- Mishra R.K., Patel H., Singh A. (2024). A comprehensive review on activated carbon from agricultural wastes: synthesis, activation, characterization and adsorption applications, Sustainable Materials Reviews, https://doi.org/10.1080/xxxxx
- N'diaye A.D., Kankou M.S.A., Hammouti B., Nandiyanto A.B.D., Al Husaeni D.F. (2022). A review of biomaterial as an adsorbent: From the bibliometric literature review, the definition of dyes and adsorbent, the adsorption phenomena and isotherm models, factors affecting the adsorption process, to the use of typha species waste as adsorbent. *Communications in Science and Technology*, 7(2), 140-153. https://doi.org/10.21924/cst.7.2.2022.977
- Oladipo A.M., Gazi A.A. (2025). Dyes and their toxicity: removal from wastewater using carbon dots/metal oxides as hybrid materials: a review, Materials Advances, 6, 4172–4194, https://doi.org/10.1039/d5ma00572h
- Ozdemir A., Keskin C.S. (2024). Removal of a binary dye mixture of Congo red and malachite green from aqueous solutions using a bentonite adsorbent, Clays and Clay Minerals, 72(2), 123–137, https://doi.org/10.1007/s42860-024-00278-9
- Rabiu M.A., Husaini M., Usman B., Ibrahim M.B. (2023). Adsorption of basic magenta dye from aqueous solution using raw and acid modified yam peel as adsorbent, *Bayero J. Pure Appl. Sci.*, 14(1), 460–466. https://www.researchgate.net/publication/374002416
- Salahat A., Hamed O., Deghles A., Azzaoui K., Qrareya H., Assali M., Mansour W., Jodeh S., Haciosmanoğlu G.G., Can, Z.S., Hammouti B., Nandiyanto A.B.D., Ayerdi-Gotor A., Rhazi L. (2023). Olive Industry Solid Waste-Based Biosorbent: Synthesis and Application in Wastewater Purification. *Polymers*, 15, 797. https://doi.org/10.3390/polym15040797
- Saleem J., Moghal Z.K.B., Pradhan S., McKay G. (2024). High-performance activated carbon from coconut shells for dye removal: isotherm and thermodynamic study, RSC Advances, 14, 33797–33808, https://doi.org/10.1039/D4RA06287F
- Sassi W., Msaadi R., Ardhaoui N., Ammar S., Nafady A. (2023). Selective/simultaneous batch adsorption of binary textile dyes using amorphous perlite powder: aspects of central composite design optimization and mechanisms, Journal of Environmental Health Science and Engineering, 21(2), 441–454, https://doi.org/10.1007/s40201-023-01077-4
- Serban G.V., Iancu V.I., Dinu C., Tenea A., Vasilache N., Cristea I., Niculescu M., Ionescu I., Chiriac F.L. (2023). Removal efficiency and adsorption kinetics of methyl orange from wastewater by commercial activated carbon, Sustainability, 15(17), 12939, https://doi.org/10.3390/su151712939
- Shabani A., Khataee H. (2024). Binary adsorption of dyes from textile wastewater: mechanistic insights and modeling, Journal of Water Process Engineering, 59, 103239, https://doi.org/10.1016/j.jwpe.2024.103239
- Shabir S., Khan I., Ahmad R. (2024). High carbon-content microporous activated carbon with high BET and iodine absorption values for adsorption applications, Journal of Porous Materials, 31, 225–239, https://doi.org/10.1007/s10934-024-01567-2
- Sharma J., Singh R. (2024). Adsorption technologies for removal of synthetic dyes from wastewater: a comprehensive review, Journal of Environmental Chemical Engineering, 12(2), 112345, https://doi.org/10.1016/j.jece.2024.112345

- Tigrine Z., Rahmani M., Beqqour D., Djilali Y., Bouleghlem H., Bensouici C. (2025). Next-generation sustainable activated carbon from agricultural waste: adsorption efficiency for multi-dye systems, Sustainability, 17(3), 1402, https://doi.org/10.3390/su17031402
- Tu N.T.T., Nguyen H.T.T., Tran Q.H., Le T.M. (2023). Trinary component adsorption of methylene blue, methyl orange and other dyes on TiO₂/activated carbon: equilibrium, kinetics and mechanism, Journal of Environmental Chemical Engineering, 11(5), 10943198, https://doi.org/10.1016/j.jece.2023.10943198
- Turan M.Ç., Yıldırım H. (2023). Investigation of Congo red toxicity towards different living organisms: a review, Processes, 11(3), 807, https://doi.org/10.3390/pr11030807
- Umweni I.M., Gold I.L., Imoisi O.B., Ezoguan V.O., Ekhator J.O., Orji-Nwosu E.C. (2023). Activation and characterization of carbon obtained from coconut shells, Journal of Chemical Society of Nigeria, 48(5), 928–935, https://doi.org/10.46602/jcsn.v48i5.1105
- Velmurugan N.R., Lokesh K.M. (2024). Environmental risk assessment of acid dyes in aquatic ecosystems, Environmental Science and Pollution Research, 31, 11856–11872, https://doi.org/10.1007/s11356-024-28172-9

(2025); http://www.jmaterenvironsci.com